Cav03-OS-6-005

Fifth International Symposium on Cavitation (Cav 2003)
Osaka, Japan, November 1 - 4, 2003

UNSTEADY PIV FLOW FIELD ANALYSIS OF A CENTRIFUGAL PUMP IMPELLER UNDER ROTATING CAVITATION

Jens Friedrichs
MTU Maintenance Hannover GmbH
Münchner Straße 31
30855 Langenhagen, Germany
E-Mail: jens.friedrichs@haj.mtu.de

Günter Kosyna
Pfleiderer-Institut für Strömungsmaschinen
TU Braunschweig, Langer Kamp 6
38106 Braunschweig, Germany
E-Mail: g.kosyna@tu-bs.de

ABSTRACT

The presented paper describes experimental investigations of rotating cavitation in centrifugal pump impellers of low specific speed with different geometries, all designed for the same operating point. All impellers are showing rotating cavitation of a very similar mechanism over a wide range of part load flow rates.

One focus of the investigations was the onset of rotating cavitation revealing an almost constant value $\sigma/2\alpha$ (cavitation number in relation to blade incidence angle) for each single impeller but a significant change between the different impeller geometries. The second part describes detailed unsteady flow field results obtained during rotating cavitation at the passage inlet as well as the outlet area. These results are giving a very good impression about the development of a cavity attached to one blade and their influence to the adjacent passage. It is shown that the interaction mechanism is mainly driven by the induced velocity distribution of the cavity affecting the flow direction (incidence angle) of the following blade. Furthermore the cavity separation as a typical vortex shedding effect and the subsequent disturbance of the entire flow within the passage caused by the vortex and its assigned wake was observed.

Finally the still remarkable influence of the vortex related disturbance at the passage outlet without any noticeable vapor content is shown with regards to the significant „creeping head drop“ of the pump.

NOMENCLATURE

b	passage width	
d	diameter	
g	gravity	
H	head	
n	impeller rotating speed	
n_s	specific speed	$333*n*\dot{V}^{1/2}/(g*H)^{3/4}$
$NPSH$	net positive suction head	$(p_s-p_v)/(\rho g)+c_s^2/(2g)$
p	static pressure	
p_v	vapor pressure	
s	blade thickness	
U	upstream mean velocity	
$\dot{V}$	volume flow	
w	impeller relative velocity	
z	number of blades	
α	incidence angle	
β	blade angle	
λ	wave-length	
ρ	density	
σ	cavitation number	$2*(p_1-p_v)/\rho U^2$
1	inlet	
2	outlet	
3%	3% pump head drop	
D	design point	
IC	incipient cavitation	
rel	design-point related	
loc	local	

INTRODUCTION

Rotating cavitation as a two-phase instability phenomenon means major impacts on performance and reliability of hydraulic pumps whenever it occurs. First discovered in inducers of high speed rocket turbopumps (Ariane-V and H-II) it has become a well known problem which has been analyzed by experimental [10] and theoretical methods [11], [13], [6]. The first observation of a similar effect in a centrifugal pump impeller was reported in [1]. During a project hosted by the DFG (Deutsche

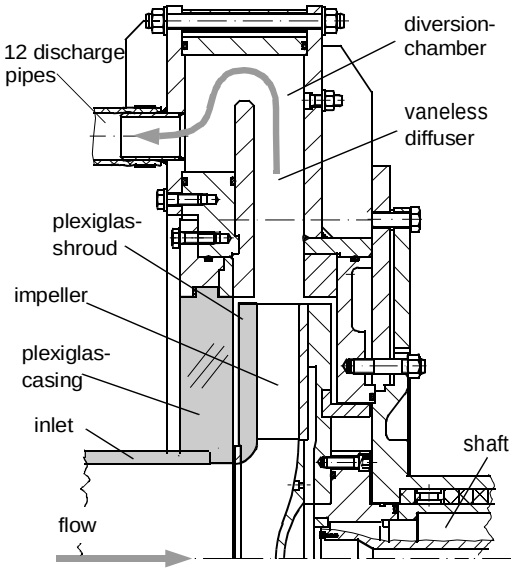

Figure 1: Cross-sectional view of test pump

Forschungsemeinschaft) and carried out by the Laboratory for Turbomachinery and Fluid Power (Technical University of Darmstadt) and the Pfleiderer-Institute (Technical University of Braunschweig) with the focus on cavitation phenomena and their erosive impacts the occurrence of rotating cavitation was again observed and confirmed in a centrifugal pump impeller of low specific speed [2]. The first visual investigations we performed to gain information about the phenomenon itself and its related effects on the overall pump performance.

The obtained results are showing a strong similarity to the turbopump phenomenon in terms of a „creeping head drop“ during rotating cavitation as well as a constant parameter $\sigma/2\alpha$ describing the onset of rotating cavitation for all operating points of one impeller geometry [3]. In addition, those investigations revealed a strong fluctuation of the passage incidence angle during rotating cavitation which was considered to be one of the driving forces leading to the rotating character of the instability.

In order to get a better understanding of the local behavior and mechanisms of rotating cavitation a detailed flow field analysis was carried out by using a customized PIV (Particle Image Velocimetry) technique. The results in terms of unsteady flow field velocity distribution during rotating cavitation allow an interpretation of the interaction between the cavity and the surrounding flow field with regards to theoretical analysis performed on turbopumps, i.e. [6]. In addition to supplement the thesis of the onset of rotating cavitation as an effect driven by the passage incidence angle two new impellers for the same design point but with a different number of blades were used for the investigation.

Impeller		**A**	**B**	**C**
Blade shape		2-circ.-arc	2-circ.-arc	2-circ.-arc
Inlet-∅	d_1	260mm	260mm	260mm
Outlet-∅	d_2	556mm	556mm	556mm
Inlet angle	β_1	17^o	19^o	20^o
Outlet angle	β_2	30^o	23^o	19^o
Passage width	b	46mm	46mm	46mm
Number of blades	z	4	5	6
Specific speed	n_s	27.5	27.5	27.5
Blade thickness	s	13mm	13mm	13mm
Rotating speed	n	9Hz	9Hz	9Hz

Table 1: Design parameters of impellers

EXPERIMENTAL SETUP

All impellers were tested in closed circuit test rig with variable system pressure. A vaneless diffuser was used instead of a volute to produce a uniform circumferential pressure distribution at the impeller outlet. The diffuser itself was connected to the upstream system by twelve discharge pipes. Figure 1 shows a cross-sectional view of the radial test pump. To enable a direct observation as well as PIV measurement of the impeller the shroud and also the front casing were made of plexiglas.

All impellers are a 2D designs with parallel shroud and hub and blades consisting of two circular arcs each. Having a different number of blades all impellers were designed for the same operating point which leads to different outlet angles as well as inlet angels. In table 1 the design parameters of all impellers are shown.

PIV Setup

In addition to the optical results shown in [2] and [3] new experimental investigations of the unsteady cavitating flow were performed using a customized PIV system. Two identical CCD cameras were mounted adjacent to each other; the first one

Laser	
Type	Nd:Yag
Thickness light-sheet	1.0 - 1.5 mm
Energy of puls	120 mJ
Puls duration	10 ns
Double-puls interval	80 - 120 µs
Camera	
Scan size	1280 x 1024 Pixel
Image size	161 x 128 mm
Focal distance	60 mm
Scale-factor	18.829
Processing	
Interrogation-area	32 x 32 Pixel
Overlapping	25 %
Subpixel interpolation	Low-pass Gaussian
Vector array size	53 x 42

Tabelle 2: PIV setup and signal processing

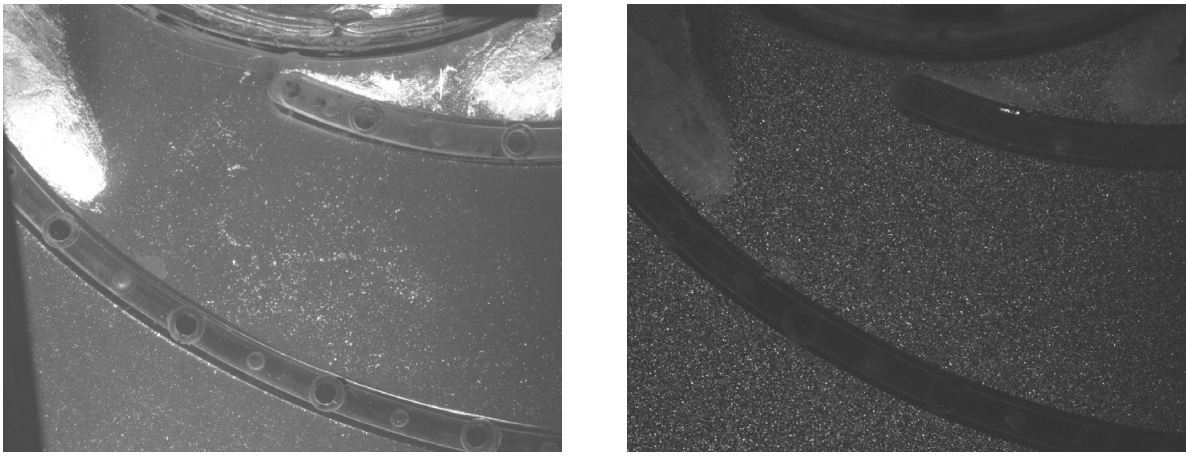

Figure 2: PIV-Images obtained at same puls: Camera 2 (532 nm, left side), Camera 1 (>570 nm, right side)

(camera 1) fitted with a low-pass filter and the second one (camera 2) with a band-pass filter. The used seeding particles were coated with Rhodamin B, a fluorescent material sending out low frequency light ($\lambda > 570nm$) once it is exposed to laser light ($\lambda \approx 532nm$). Since the seeding is carried by the liquid phase of the cavitating flow the low-pass filtered camera 1 is observing only this liquid phase and it is not disturbed by the bright reflections coming from the vapor/liquid phase transition.
On the other hand camera 2 operating with the band-pass filter can be adjusted to the directly reflected laser light (lower shutter) to obtain images from the unsteady vapor/liquid distribution of exactly the same state. Both cameras are taking double exposure images (double laser puls) at the same time.
During the following signal processing the images from camera 1 are cross-correlated leading to a local displacement vector field of the liquid phase. In parallel one image from camera 2 is used to record the vapor/liquid distribution of the flow for the same laser puls. In figure 2 two typical images obtained by this method are shown. On the left hand (camera 2) the typical phase distribution of full developed rotation cavitation can be found characterized by a large cavity area consisting of multiple phase limits. The same laser puls as it is seen by camera 1 on the right hand: A uniform seeding distribution can be found within the liquid flow as a major requirement for the following cross-correlation without disturbance from the cavity area which appears more as a faded zone. Table 2 shows the main parameters of the used PIV system. In addition to the cross-correlation analysis all flow field images were validated using a moving average validation [7] and finally transferred from the PIV absolute system into the impeller relative system:

$$\overrightarrow{w_{loc}} = \overrightarrow{c_{loc}} - \overrightarrow{u_{loc}}$$

RESULTS AND DISCUSSION

Overall performance and instability

As a major requirement to allow a comparison of the impellers A, B and C with regards to rotating cavitation the overall performance of the impellers within the test pump (Fig.1) was checked. Since all impellers were designed based on the same theory [9] a good coincidence within the pressure rise as well as the efficiency was found, see [4]. The second important comparison in terms of NPSH at incipient cavitation and 3% pump head drop is shown in fig. 3. Starting with $NPSH_{IC}$ a very similar behavior can be seen which confirms the design point for all impellers by the onset of bubble generation at the impeller inlet due to local pressure drop.
The $NPSH_{3\%}$ results are also very similar with regards to the shape of the curves and the position of their minima. One small

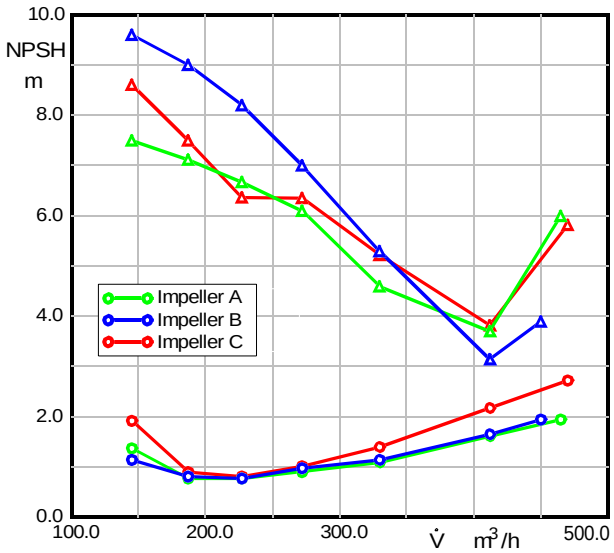

Figure 3: $NPSH_{IC}$ und $NPSH_{3\%}$ for different impellers

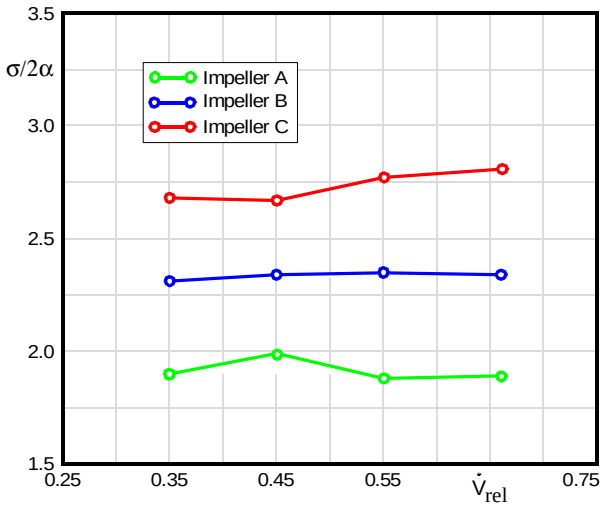

Figure 4: Onset off rotating cavitation

difference can be seen within the increase of $NPSH_{3\%}$ for impeller C on both sides of its minimum. Taking into account the same blade thickness for all impellers the blockage at the inlet during cavitation as the sum of blade and cavity caused blockage is increased for a higher number of blades which explains the observed behavior.

Focussing on rotating cavitation fig. 4 shows the onset of the instability for the tested configurations. All impellers are showing the phenomenon at part load conditions of 66% design flow rate and below. For the 5-bladed impeller (Impeller B) the observation was already discussed in [2] where also a comparison with a scaled pumps and different leading edge geometries was shown. In terms of σ/2α both pumps revealed the beginning of rotating cavitation at the same time.
Therefore the conclusion was drawn that rotating cavitation can be understood as an impeller instability problem which is driven by the relation of increasing cavity volume (or cavity length) and impeller incidence angle.
By extending the analysis with the results of impeller A and C this explanation is completely confirmed. Both new impellers are showing in each case an almost constant onset of rotating cavitation expressed in σ/2α for all flow rates. But the level is shifted of approximately 0,42 compared to impeller B, downwards for the 4-bladed impeller (Imp. A) and upwards for the 6-bladed (Imp. C).
Since the change of the incidence angle as the difference between design point and actual flow angle is the same for all impellers at the same flow rate, the shift of σ/2α must be caused by a shift of σ meaning the onset of rotating cavitation at a different system pressure.
From the observation during rotating cavitation it was found that the shape of the cavity during onset and fully developed rotating cavitation is the same for all impellers at the same flow rate, which is also major driven by the described incidence angle. Therefore the observed shift in σ/2α is not caused by a changed type of cavitation but by a geometrically similar cavity of different size.
In terms of the interaction between cavity and impeller passage this can be explained as a larger cavity (lower σ) which is required to cause the same instability for impeller A due to its larger pitch (t) or, on the other hand a smaller cavity (higher σ) to cause the same instability for impeller C with a smaller pitch.

Based on σ/2α = 2,35 as the results for impeller B the shift of impeller A and C in fig. 4 is approximately +/- 17%. Transferring the impeller design into a 2-dimensional cascade model a shift within the pitch of +/- 20% for A and C compared to B can be found.
This means according to the results of [12] and [6] the cavity size related to the pitch of the cascade is the important instability criteria for development of rotating cavitation.

Unsteady flow field at impeller inlet

In order to analyze the detailed behavior of the flow in one passage during a sequence of rotating cavitation fig. 5 to 9 show the results obtained by using the above described PIV technique. Each figure shows the inlet of the same passage of impeller B after different revolutions within the same sequence of rotating cavitation. In order to allow a most detailed analysis within one sequence of rotating cavitation a operating point of low propagation velocity was chosen, in this case approx. 9-10 impeller revolutions for a full sequence.
In the upper half of the figures the unsteady flow field result (left) in combination with the vapor/liquid distribution (right) can be seen. In addition a detailed view of the blade leading edge at the same state is shown (bottom left) were red arrows derived from the average non-cavitating flow are fitted to allow an interpretation of the unsteady local behavior of the blade incidence angle. The two plots of normal velocity (w_{normal}) contain the distribution of the relative velocity normal to the sketched lines I and II. For each state the unsteady distribution (red) is compared with an average non-cavitating distribution (grey dotted). The local relative flow rate ($\dot{V}_{loc,\,rel}$) indicates the unsteady through flow at plane I and II divided by the non-cavitating value.

$$\dot{V}_{loc,\,rel} = \frac{\int w_{normal,\,i} \cdot (k)\,dk}{\int w_{normal,\,non-cav} \cdot (k)\,dk}$$

Starting at fig. 5 no cavitation is visible within the observed passage while on the suction side of the following blade a large cavity can be seen. The velocity distribution in the passage is quite uniform and the relative velocities at plane I and II indicate a local flow condition similar to the non-cavitating state which can also be seen within the detailed leading edge view.
Three revolutions later (state 2) the same passage is shown in fig. 6. Within these revolutions a cavity has developed at the

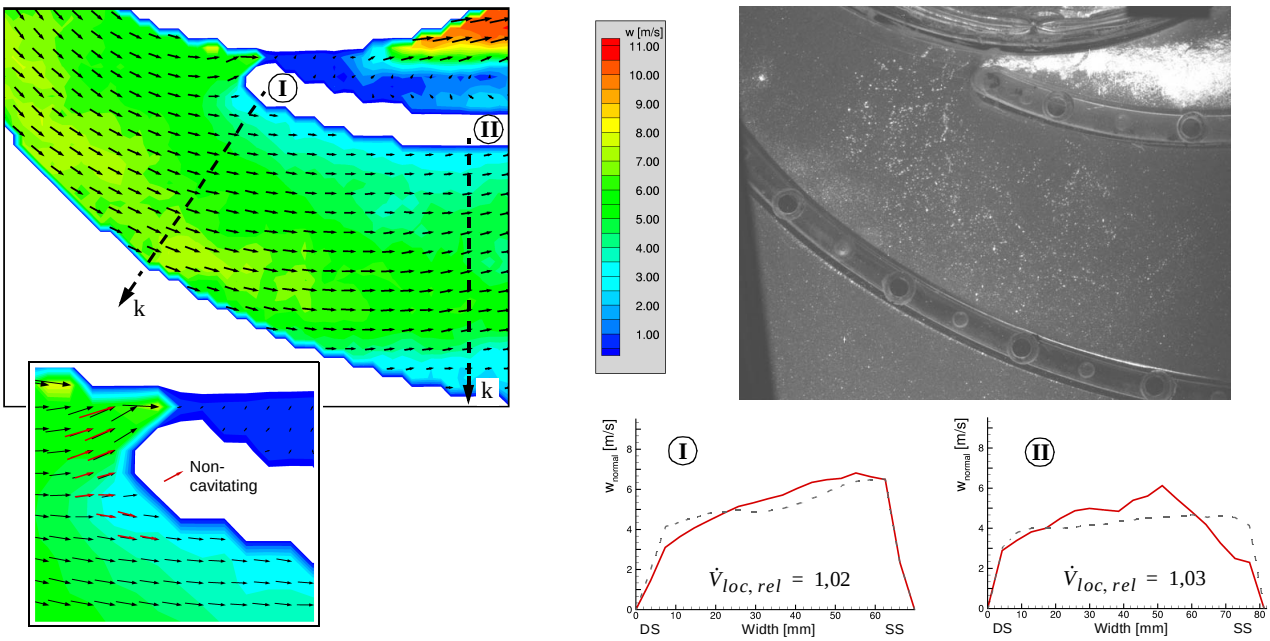

Figure 5: Rotating cavitation at impeller B at 45% flow rate (State 1)

blade ahead (lower blade). Parallel to the increasing size of this cavity the cavity of the following blade has become smaller as also described in [2]. For the shown state the first cavity originating from the blade ahead is still in front of the passage inlet. Nevertheless the direction of the flow in front of the following blades indicates a significant difference from the non-cavitating state in terms of a local decreased incidence angle. This observation explains the changed shape of the cavity of the following blade, meaning a shorter length as well as a smaller angle between blade surface and phase limit as an indication for the local flow angle. The normal velocities at I and II are indicating a distribution still similar to the non-cavitating flow with an increased through flow of about 10% in the passage. This shows that the mechanism of rotating cavitation cannot only be explained by pure blockage effects. Although the cavity in front of the passage should mean reasonable geometrical blockage the through flow of the passage is increasing and the following blade leading edge also shows an decreased incidence angle.

This indicates a mechanism which is driven by induced velocities caused by the flow around the cavity similar to the description given in [6]. In fig. 7 just one revolution later the cavity has entered the passage. The through flow at I and II has dropped significantly showing a completely changed distribution at plane I with increased velocities near the pressure side of the following blade and back flow at the pressure side of the passage. At plane II a drop can be found near the pressure side of the following blade. Within the cavity itself a vortex structure is visible showing the zone of forward flow outside the cavity and back flow inside divided by a distinct cavity closure region with an indicated stagnation point on the blade surface. At the leading edge of the following blade a difference of approx. 50° between the unsteady state flow direction and non-cavitation flow can be found. This rapid decrease means a significant change in the blade velocity and pressure distribution leading to an almost completely vanished cavity on suction side in combination with a beginning separation on the pressure side of this blade.

Another three revolutions later (state 4) in fig. 8 two separated vortex structures have developed out of the attached cavity of fig. 7 (remark: generation of two vortices is not typical, also a single vortex generation was observed). Both vortices are carrying a zone of decreased relative velocity or even local back flow near the passage suction side in combination with an overspeed zone near the pressure side. While the velocity distribution at I is dominated by this vortex structures, the distribution at II clearly indicates the separation of the flow at the following blade pressure side which can also be seen in the flow field. This separation is a consequence of the rapid decrease in the local flow incidence angle as shown in fig. 7. In the meantime the incidence angle has slightly increased resulting from the less overspeed between cavity and following blade.

The following state 5 in fig. 9 shows a remarkable decrease of the vapor content within the passage as a consequence of the increased downstream pressure level. Nevertheless the disturbance of the flow within the passage caused by the vortex structures near the suction side is still noticeable.

With the vortex structure proceeding downstream the velocity at plane II is also changed to higher flow near the pressure side and

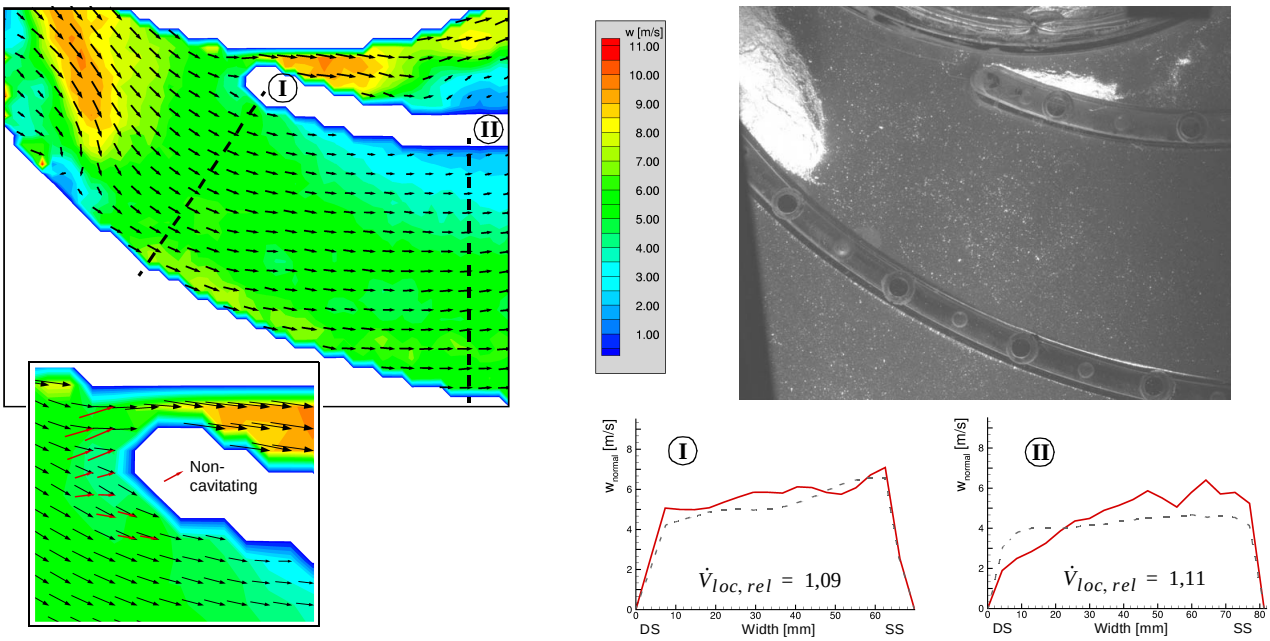

Figure 6: Rotating cavitation at impeller B at 45% flow rate (State 2)

lower flow near the suction side. For the propagation velocity of the vortex structure itself the values obtained from the PIV measurement of 10 - 15 cm per revolution are matching the average displacement of the structure between different revolutions.

In the following states (not shown) the vapor structure is moving further downstream and at the same time the velocity distribution as well as the leading edge flow direction are developing back to the non-cavitating state for this passage. This development means an increased incidence angel for the following blade and therefore the growth of its suction side cavity which then means a state like it is shown in fig. 6 and 7 for the first blade.

Thus the following blade is showing a time-shifted sequence of the same cavity development, leading to rotating cavitation for the whole impeller while the „link“ between the passages is defined by the unsteady incidence angle development.

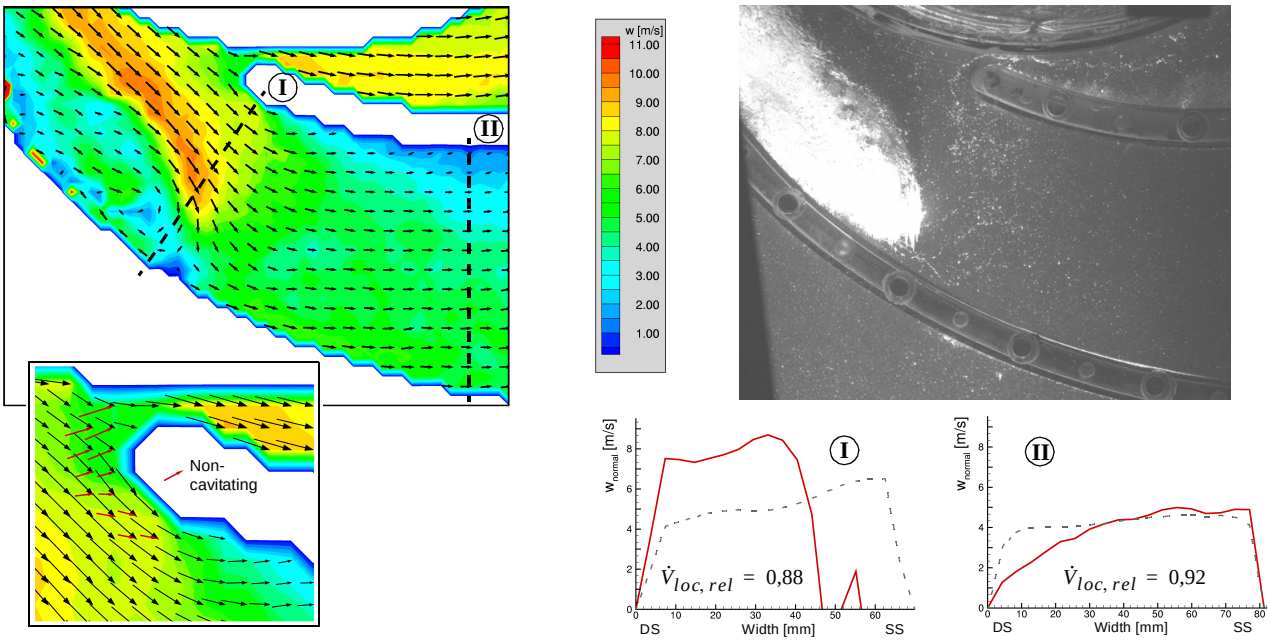

Figure 7: Rotating cavitation at impeller B at 45% flow rate (State 3)

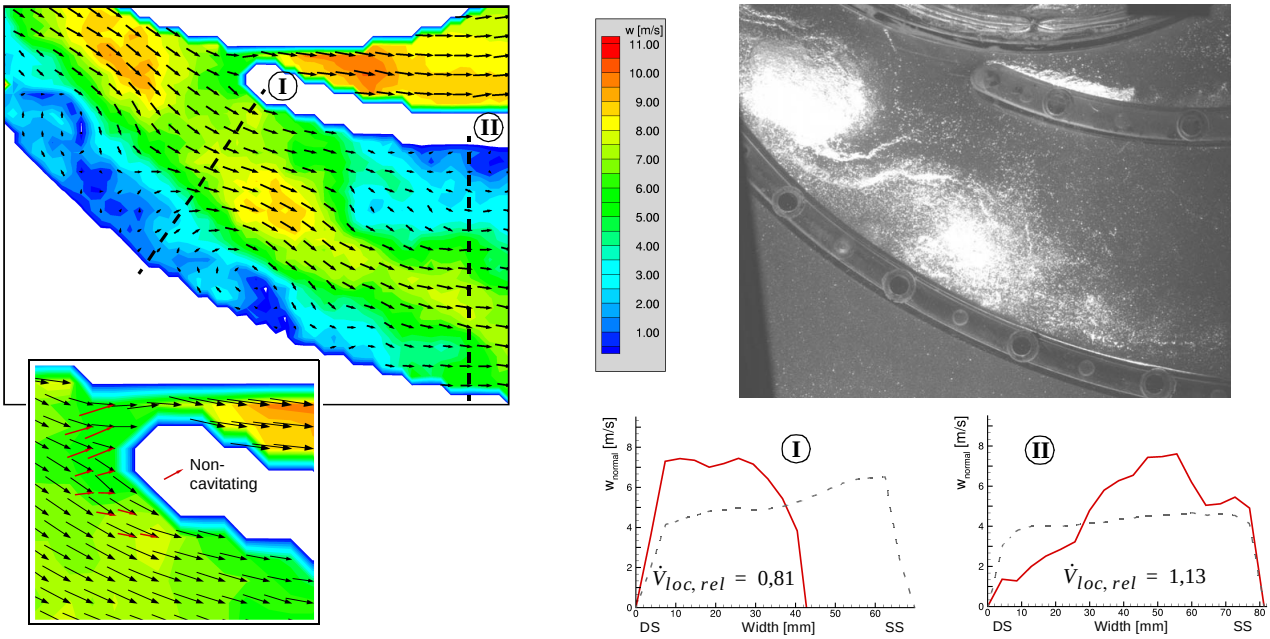

Figure 8: Rotating cavitation at impeller B at 45% flow rate (State 4)

Furthermore the different observed states during the sequence are showing a remarkable similarity compared to the analytical results of [8]. Especially within the vapor/liquid phase distribution of single states of very similar character can be obtained pointing out the also similar driving mechanism with regards to the incidence angle.

Unsteady flow field at passage outlet

While the main mechanism of rotating cavitation is driven by the interaction at the passage inlet, the pumping head and therefore also the head drop of a centrifugal pump is mainly defined by the flow conditions at passage outlet. Since the rotating cavitation was identified to have a significant impact not only on pump performance but also on cavitation noise and

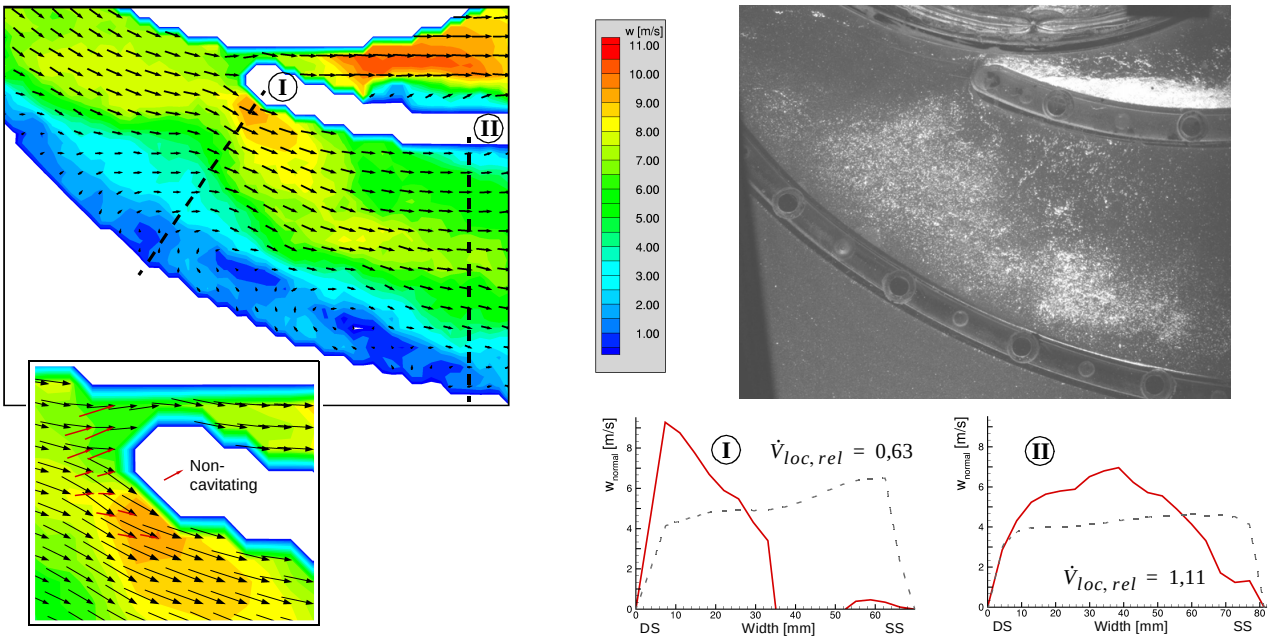

Figure 9: Rotating cavitation at impeller B at 45% flow rate (State 5)

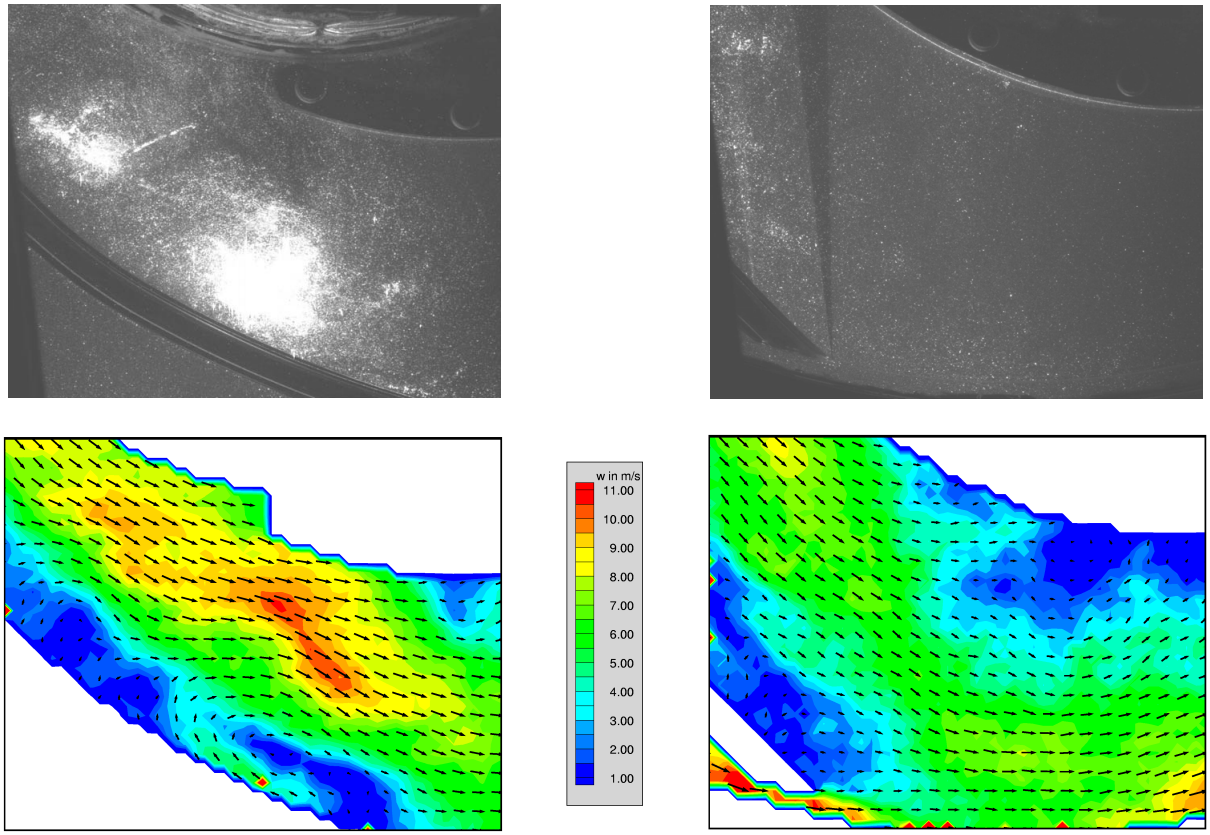

Figure 10: Rotating cavitation at impeller A at 45% flow rate (left: inlet, right: outlet)

erosion, the passage outlet was investigated under rotating cavitation conditions using again the PIV setup.

Fig. 10 shows the inlet and outlet area of one passage of impeller A during rotating cavitation. Both states (left and right) are single shot images at the same operating point but from different sequences of fully developed rotating cavitation.

At the impeller inlet (left) a typical vortex separation similar to the one analyzed above can be found within the observation as well as the PIV result. At the outlet (right) the vapor content of the flow is reduced to small single bubbles indicating no significant disturbance. But the still present impact of rotating cavitation to the entire flow in the passage is demonstrated by the PIV result. Near the trailing edge of the first blade a clearly defined vortex structure is still visible. This structure, originating from a former cavity separation near the leading edge of the same blade (as described above) has been transported downstream by the main flow as a distinct feature which still means a remarkable disturbance of the surrounding flow in terms of blockage and induced velocities.

Thus not only the direct consequences of cavitation as bubble generation and collapse but also the persistence of the separated vortex structure and its wake are playing a major role during rotating cavitation, especially with regards to the pump performance.

Furthermore also a separated zone a the pressure side of the following blade can be seen. These zone is also a typical observation at the passage outlet during rotating cavitation appearing alternating to the described suction side vortex. By comparing this separation with fig. 8 a similar zone at the pressure side of the following blade can be found caused by the cavity induced velocity distribution in the passage inlet area. After once generated at the inlet these pressure side separation zone seems to be continuously driven be the suction side cavity vortex structure. An observation of one passage outlet during rotating cavitation reveals a flow which is permanently impressed by alternating separation zones at both sides of the passage. Thus no steady flow similar to the non-cavitating state can develop.

On the other hand the still visible vapor fraction near the passage outlet means that at least one portion of the vapor volume is transported far downstream where the bubble collapse is driven by a significantly higher pressure gradient than normal. This means that not only the cavitation noise but also the erosive impact is increased.

CONCLUSIONS

The presented paper describes detailed experimental results obtained during rotating cavitation. Based on preceding observations of the phenomenon in a centrifugal impeller of low specific speed the experiments were extended to modified impeller geometries as well as detailed flow field investigations.

Using the new impeller geometries a significant change in the onset of rotating cavitation was observed in terms of a shift in $\sigma/2\alpha$ for different blade numbers while each impeller itself was showing a constant $\sigma/2\alpha$ for all flow rates. In addition the phenomenon of rotating cavitation itself obtained a very similar character for all impellers. By considering the modified passage inlet geometric was shown that the instability limit is defined by a critical cavitation number in relation to the passage throat area. The described shift in $\sigma/2\alpha$ is therefore reflecting the changed cavity size (σ) required to generate the same instability.

By using an adapted PIV system a detailed unsteady flow field investigation of the rotating cavitation cycle was performed. The obtained results confirmed the interaction between the cavity of one blade and the leading edge (throat area) of the following blade as the driving reason for rotating cavitation. Within these mechanism it is not only the pure blockage effect caused by the cavity which influences the flow but mainly the induced velocity field of the cavity including their wake. Especially the incidence angle of the following blade which can be considered to be the link between the unsteady behavior of one cavity and the increasing or decreasing cavity of the following blade is highly driven by the velocity and direction of the flow above the cavity.

During separation of the cavity as a typical vortex shedding mechanism it was shown that a distinct vortex structure is formed and subsequently carried down the passage by the main flow. These vortex structure and thus the related wake were found to be very stable on their way downstream even if the entire bubble/vapor content has already collapsed. Therefore a severe disturbance of the passage outlet flow described by alternating separation zones on both sides of the passage was recognized as the reason for the pump head drop during rotating cavitation.

ACKNOWLEDGMENTS

The presented study was carried out in cooperation with DFG (Deutsche Forschungsgemeinschaft).

REFERENCES

[1] Dreiß, A., 1997, „Untersuchung der Laufradkavitation einer radialen Kreiselpumpe durch instationäre Druckmessung im rotierenden System“, *Mitteilungen des Pfleiderer.-Instituts 5, Verlag und Bildarchiv W.H. Faragallah.*

[2] Friedrichs, J., Kosyna, G., Hofmann, M., Stoffel, B., 2001, „Similarities and Geometrical Effects on Rotating Cavitation in Two Scaled Centrifugal Pumps“, *Proceedings of CAV 2001, Pasadena.*

[3] Friedrichs, J., Kosyna, G., 2002, „Rotating Cavitation in a Centrifugal Pump Impeller of Low Specific Speed“, *ASME Journal of Fluids Engineering, Vol. 124,* pp. 356-362.

[4] Friedrichs, J., 2003, „Auswirkungen instationärer Kavitationsformen auf Förderhöhenabfall und Kennlinieninstabilität von Kreiselpumpen“, *Mitteilungen des Pfleiderer.-Instituts 9, Verlag und Bildarchiv W.H. Faragallah.*

[5] Hofmann, M., 2001, „Ein Beitrag zur Reduzierung der erosiven Aggressivität kavitierender Strömungen“, *Dissertation TU Darmstadt.*

[6] Horiguchi, H., Watanabe, S., Tsujimoto, Y., Aoki, M., 2000, „A Theoretical Analysis of Alternate Blade Cavitation in Inducers”, *ASME Journal of Fluids Engineering, Vol. 122,* pp. 156-163.

[7] Host-Madsen, A., McCluskey, D.R., 1994, „On the Accuracy ans Reliability of PIV Measurements“, *Proc. of the 7th Int. Symp. on Appl. of Laser Techniques to Flow Measurements, Lisbon.*

[8] Iga, Y., Nohmi, M., Goto, A., Shin, B.R., Ikohagi, T., 2002, „Numerical Analysis of Unstable Phenomena of Cavitation in Cascade with Finite Blade Numbers“, *9th Int. Symp. on Transport Phenomena and Dynamics of Rotating Machinery, Honolulu, Hawaii.*

[9] Traupel, W., 1962, „Die Theorie der Strömung durch Radialmaschinen“, *Verlag G. Braun, Karlsruhe.*

[10] Tsujimoto, Y., Yoshida, Y., Maekawa, Y., Watanabe, S., Hashimoto, T., 1997, „Observations of Oscillating Cavitation of an Inducer”, *ASME Journal of Fluids Engineering, Vol. 119,* pp. 775-781.

[11] Tsujimoto, Y., Kamijo, K., Yoshida, Y., 1993, „A Theoretical Analysis of Rotating Cavitation in Inducers”, *ASME Journal of Fluids Engineering, Vol. 115,* pp. 135-141.

[12] Tsujimoto, Y., 2001, „Simple rules for Cavitation Instabilities in Turbomachinery“, *Invited lecture, Cavitation symposium, Cav2001, Pasadena*

[13] Watanabe, S., Sato, K., Tsujimoto, Y., Kamijo, K., 1999, „Analysis of Rotating Cavitation in a Finite Pitch Cascade Using a Closed Cavity Model and a Singularity Method”, *ASME Journal of Fluids Engineering, Vol. 121,* pp. 834-840.